TR 89010
OCTOBER

Final Report

# NOVEL IN SITU SPECTROSCOPIC ELLIPSOMETER FOR REAL TIME ANALYSIS OF CVD DIAMOND FILMS

Prepared by:

Diamond Materials, Inc.
2820 East College Avenue
State College, PA 16801

Principal Investigator:

Dr. Richard Koba

Prepared for:

Defense Advanced Research Projects Agency (DoD)
Defense Small Business Innovation Research Program
ARPA Order Number ACN RD942
Issued by U.S. Army Missile Command Under
Contract Number DAH01-88-C-0899



Diamond Materials Institute

# REPORT DOCUMENTATION PAGE

| | |
|---|---|
| 1a REPORT SECURITY CLASSIFICATION<br>Unclassified | 1b RESTRICTIVE MARKINGS |
| 2a SECURITY CLASSIFICATION AUTHORITY | 3 DISTRIBUTION/AVAILABILITY OF REPORT<br>Approved for public release; distribution unlimited. |
| 2b DECLASSIFICATION/DOWNGRADING SCHEDULE | |
| 4 PERFORMING ORGANIZATION REPORT NUMBER(S) | 5 MONITORING ORGANIZATION REPORT NUMBER(S) |
| 6a NAME OF PERFORMING ORGANIZATION<br>Diamond Materials, Inc. — 6b OFFICE SYMBOL (If applicable) | 7a NAME OF MONITORING ORGANIZATION<br>U.S. Army Missile Command |
| 6c ADDRESS (City, State, and ZIP Code)<br>2820 East College Avenue<br>State College, PA 16801 | 7b ADDRESS (City, State, and ZIP Code)<br>DARPA Project Office<br>AMSMI-RD-DP-TT<br>Redstone Arsenal, AL 35898-5280 |
| 8a NAME OF FUNDING/SPONSORING ORGANIZATION<br>DARPA — 8b OFFICE SYMBOL (If applicable) | 9 PROCUREMENT INSTRUMENT IDENTIFICATION NUMBER<br>DAAH01-88-C-0899 |
| 8c ADDRESS (City, State, and ZIP Code)<br>1400 Wilson Blvd.<br>Arlington, VA 22209-2308 | 10 SOURCE OF FUNDING NUMBERS<br>PROGRAM ELEMENT NO. / PROJECT NO. / TASK NO. / WORK UNIT ACCESSION NO |

11 TITLE (Include Security Classification)
Novel In-Situ Spectroscopic Ellipsometer for Real Time Analysis of CVD Diamond Films

12 PERSONAL AUTHOR(S)
Koba, Richard J.

| 13a TYPE OF REPORT | 13b TIME COVERED | 14 DATE OF REPORT (Year, Month, Day) | 15 PAGE COUNT |
|---|---|---|---|
| Final | FROM 88/9/30 TO 89/8/30 | 1989, October 4 | |

16 SUPPLEMENTARY NOTATION

| 17 COSATI CODES | | | 18 SUBJECT TERMS (Continue on reverse if necessary and identify by block number) |
|---|---|---|---|
| FIELD | GROUP | SUB-GROUP | Spectroscopic ellipsometry, carbon allotropes, PECVD diamond, in-situ |
| | | | |
| | | | |

19 ABSTRACT (Continue on reverse if necessary and identify by block number)

Diamond Materials, Inc. (DMI), has designed and assembled a split reflected beam spectroscopic ellipsometer (SRBSE) and has performed ellipsometric measurements on four different samples. The four samples were: (1) a bare silicon wafer, (2) a silicon wafer coated with diamond-like carbon, (3) a silicon wafer coated with diamond over 70% of its surface area, and (4) a silicon wafer coated with a fully dense diamond film. The purpose of the Phase I program was to determine whether SRBSE could distinguish between different carbon films deposited on silicon substrates, thereby serving as a low-cost alternative to more expensive spectroscopic techniques. Design of the SRBSE and analysis of the experimental data was performed with the assistance of the consultant on this Phase I program, Dr. O. Louis Russo of the New Jersey Institute of Technology. Dr. Russo is the inventor of SRBSE.

After months of design changes and equipment upgrades, the SRBSE could not provide accurate ellipsometric results over the range of light wavelengths investigated. The SRBSE could distinguish a coated substrate from an uncoated substrate. However, the measurements were too inaccurate to distinguish between the various types of carbon coatings on silicon. The lack of accuracy was attributed

| 20 DISTRIBUTION/AVAILABILITY OF ABSTRACT | 21 ABSTRACT SECURITY CLASSIFICATION |
|---|---|
| ☒ UNCLASSIFIED/UNLIMITED ☐ SAME AS RPT. ☐ DTIC USERS | Unclassified |
| 22a NAME OF RESPONSIBLE INDIVIDUAL | 22b TELEPHONE (Include Area Code) / 22c OFFICE SYMBOL |

to sensitivity of SRBSE to slight changes in optical beam alignment, polarization, and monochromaticity of the incident beam. Two important conclusions were drawn from the Phase I program:

1. The required hardware configuration of a SRBSE instrument is dependent upon the type of sample being examined. The shape of the pyramidal beam splitter is dictated by the optical properties of the substrate upon which films are deposited and, to a lesser extent, the optical properties of the films themselves. Therefore, the SRBSE built in this program was suited only for the analysis of thin films on single crystal Si substrates. A different beam splitter would have to be machined for examining films on different substrates.

2. A major reason for measurement error was the insufficiently strong beam intensities despite the fact all measurements were made under carefully controlled conditions designed to maximize the sensitivity of light detection. Therefore, it is concluded that SRBSE (using the light source + monochrometer arrangement examined here), is not suited for *in situ* measurement of any thin-film deposition processes. Since inaccuracies arose under the idealized conditions examined in Phase I, additional difficulties arising from *in situ* measurements, e.g., the use of windows on vacuum chambers and background signal from PECVD plasmas, renders SRBSE unsuitable for *in situ* applications.

After the time and money spent on this Phase I program, SRBSE was not able to replicate the results of commercial, albeit more expensive, spectroscopic ellipsometers. The benchtop model SRBSE could not achieve accurate results due to extreme sensitivity of the technique to instrumental factors; therefore, SRBSE shows little or no promise for *in situ* characterization. Because of these conclusions, Diamond Materials, Inc., has declined to submit a proposal for a Phase II, follow-on program.

TR 89010
OCTOBER

Final Report

# NOVEL IN SITU SPECTROSCOPIC ELLIPSOMETER FOR REAL TIME ANALYSIS OF CVD DIAMOND FILMS


Contractor: Diamond Materials, Inc.
2820 East College Avenue
State College, PA 16801



Effective Date of Contract: September 30, 1988

Contract Expiration Date: March 30, 1989

Reporting Period: September 30, 1988 to September 30, 1989

Date of Final Report: October 4, 1989



Principal Investigator: Dr. Richard Koba

Telephone Number: (814) 231-6200



Sponsored by:

Defense Advanced Research Projects Agency (DOD)
Defense Small Business Innovation Research Program
ARPA Order Number ACN RD942
Issued by U.S. Army Missile Command Under
Contract Number DAH01-88-C-0899

Certification

Contractor, Diamond Materials, Inc., hereby certifies that to the best of its knowledge and belief the technical data delivered herewith under contract number DAAH-01-88-C-0899 is complete, accurate and complies with all requirements of the contract.

Date October 3 1987

Name and Title of Certifying Official:

Richard Koba

Richard Koba
Principal Investigator
Materials Scientist

TABLE OF CONTENTS

# 1. INTRODUCTION

The purpose of this SBIR Phase I program was to design, assemble, and qualify a novel surface analysis instrument known as a split reflected beam spectroscopic ellipsometer, SRBSE. The SRBSE was used to see if it could distinguish between a diamond and diamond-like carbon film deposited on silicon substrates. Research into the utilization of SRBSE was motivated by two reasons:

1. SRBSE promised to be significantly less expensive than conventional methods of distinguishing between diamond and diamond-like thin films, namely, Raman spectroscopy or conventional spectroscopic ellipsometry.

2. Because of the relatively low cost of SRBSE and its supposed high sensitivity to carbon films, it was hoped that such instruments could be mounted on CVD deposition chambers to permit *in situ* measurements of film coatings.

The consultant of this Phase I program was the inventor of SRBSE, Dr. O. Louis Russo. The invention of SRBSE was announced in a paper published in 1985; to Dr. Russo's knowledge, no one other than he has replicated his initial work [1]. The goal of this Phase I program was to replicate SRBSE outside of Dr. Russo's laboratory and qualify the instrument to see if it could distinguish between diamond-like carbon and diamond films.

The suitability of ellipsometry as a method for *in situ* spectroscopic examination during CVD is already been recognized for diamond-like film deposition [2]. K. Vedam and R. W. Collins at Penn State University are leading a research effort into performing spectroscopic ellipsometry *in situ* during the growth of diamond and diamond-like carbon films. However, the Penn State group is utilizing a sophisticated computer controlled spectroscopic ellipsometer, worth over $150,000, which was designed and built by the commercial French firm *Sopra*. The initial results of spectroscopic ellipsometry analysis of carbon films is described in very recent publications [3,4]. The sophisticated instrument built by Sopra can allow spectroscopic data to be collected over all visible wavelengths in under two seconds. The Sopra unit also has optics which are robust enough to enable *in situ* measurement in small, custom built CVD chambers. However, despite three years of intensive work using a highly sophisticated instrument manned by at least four full-time graduate students, preliminary results from the Penn State group are only just now being submitted for

publication. The PSU ellipsometry research group has demonstrated that spectroscopic ellipsometry of carbon films is a difficult, time consuming and expensive endeavor in order to achieve reliable results.

The advantages of ellipsometry as a method of *in situ* analysis are clear [4]. Ellipsometry can employ near-ultraviolet, visible or near-infrared light to obtain optical data about a sample over a broad spectral range. Ellipsometry collects data by measuring changes in the polarization and phase angle of light as it is bounced off a surface. Therefore, the technique requires light propagation plus reflection off a surface. *In situ* ellipsometry can be performed in a thin-film deposition chamber at a variety of gas pressures, corrosive ambients, and a variety of substrates.

Ellipsometry provides information about the complex dielectric response of a sample material. Complex dielectric response can be expressed either as the complex dielectric function $\varepsilon^*$ or, for the purposes of this report, the complex refractive index $n^*$ defined as $n^* = n(1 - i\kappa)$ where n is the real refractive index, $\kappa$ is the imaginary refractive index, and the product $n\kappa$ is defined as the absorption coefficient k. For clear, non-absorbing materials, $k = 0$ and $n^2 = \varepsilon = \varepsilon^*$.

Ellipsometric data is processed according to Fresnel's equations. The final results provide the real and imaginary refractive index of either a bare substrate or a substrate coated with a homogeneous thin-film coating. If the optical constants of the substrate are well known, the ellipsometric data is typically used to extract the refractive index (both real and imaginary) as well as the thickness of the thin-film coating. One of the major limitations of ellipsometry as a method to measure thickness is that the data provides only for reporting the $0^{th}$ order thickness, $t_0$, plus a thickness increment $\Delta t$ where the final true thickness is expressed as $t_0 + m\Delta t$ where m is an integer. Ellipsometric data alone cannot determine the value of m. In that respect, ellipsometry is similar to hitting a note on a piano. It can tell you the name of the note (A, B, C, E-flat, etc.), but it cannot determine the octave from which the note was produced. Hence, ellipsometry's greatest utility is for very thin films where value of the integer m is known to be 0,1 or 2.

Ellipsometric data is difficult to analyze without the use of a computer program which can handle complex number mathematics required by Fresnel's equations. For this Phase I program, DMI's consultant, Dr. Russo, was responsible for the processing of all experimental data. Unfortunately, Dr. Russo did not have access to a sophisticated computer program. Therefore, most of the experimental data was processed manually. Manual data processing was very time consuming, and limited the number of samples

whose ellipsometric data could be processed. Therefore, ellipsometric measurements were made on a total of four samples described as follows:

1. A bare silicon wafer oriented (100).

2. A silicon wafer deposited with a coating of diamond-like carbon, thickness below 0.5 μm.

3. A silicon wafer coated with a layer of polycrystalline diamond which covered only 70% of the surface of the silicon. The other 30% of the surface was porosity. The diamond regions were ≈ 3.2 μm thick.

4. A silicon wafer coated with a dense polycrystalline diamond coating ≈ 2.9 μm thick.

## 2. EXPERIMENTAL PROCEDURES

### 2.1 Design and Assembly of the Split Reflective Beam Spectroscopic Ellipsometer

A schematic diagram of the SRBSE is shown in Figure 1. Figure 2 illustrates the nomenclature used to define the E-field orientation of the polarizer and the two analyses. Figures 3 through 6 are photographs showing various portions of the SRBSE. The following description of the SRBSE traces the path of the light beam.

The light source was a McPherson dual light source containing both a tungsten lamp and a deuterium lamp. The two light sources together can emit wavelengths between 200 nm and 600 nm. Use of UV light ($\lambda < 400$ nm) was problematic due to significant changes in focal length over the UV wavelengths. Therefore, no meaningful measurements could be made at wavelengths shorter than 400 nm; all measurements performed in this Phase I program utilized visible wavelengths.

The exit aperture of the McPherson light source was connected to the entrance aperture of a Bausch and Lomb monochrometer. The monochrometer was fitted with a 1200 groove/mm grating. After experimentation, it was found that the light emerging from the monochrometer needed to be diffused to eliminate elliptical polarization. The most effective light diffuser turned out to be scotch tape which was affixed over the exit slit of the monochrometer.

Since the beam emerging from the monochrometer had a divergence angle of 17°, a lens system was employed to collimate the beam. Plano-convex lenses were used for collimation, as shown in Figure 5. The collimated beam was then directed through an Oriel transmission polarizer. The E-field direction of the polarizer was situated always at an angle of + 45° according to the convention described in Figure 2. The purpose of this polarizer was to try to depolarize the beam incident on the substrate. The SRBSE technique required completely depolarized light to be incident on the substrate. However, use of a grating monochrometer automatically polarized the beam with the E-field situated at + 90°, that is, vertically. Therefore, insertion of a + 45° polarizer was designed to depolarize the beam.

After the Oriel polarizer, the light was then directed onto the surface of the substrate. All substrates were mounted vertically on a precision substrate holder. As illustrated in Figure 6, the substrate holder was placed along the axis of a gear which was part of a gear mechanism designed to ensure that the reflected light off the surface of the substrate was always directed into the beam splitter (the aluminum pyramid).

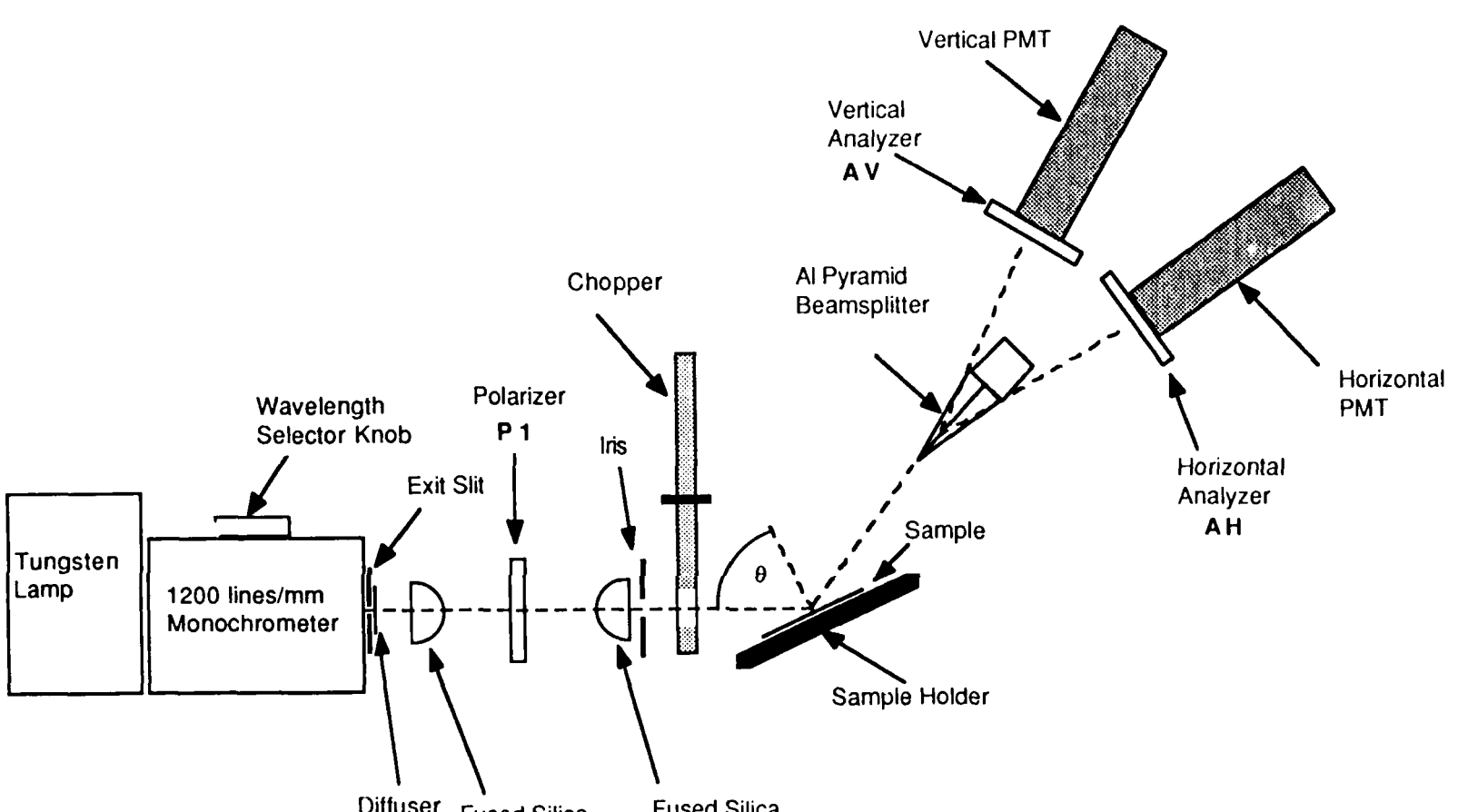


FIGURE 1. SCHEMATIC OF THE SRBSE (NOT TO SCALE).

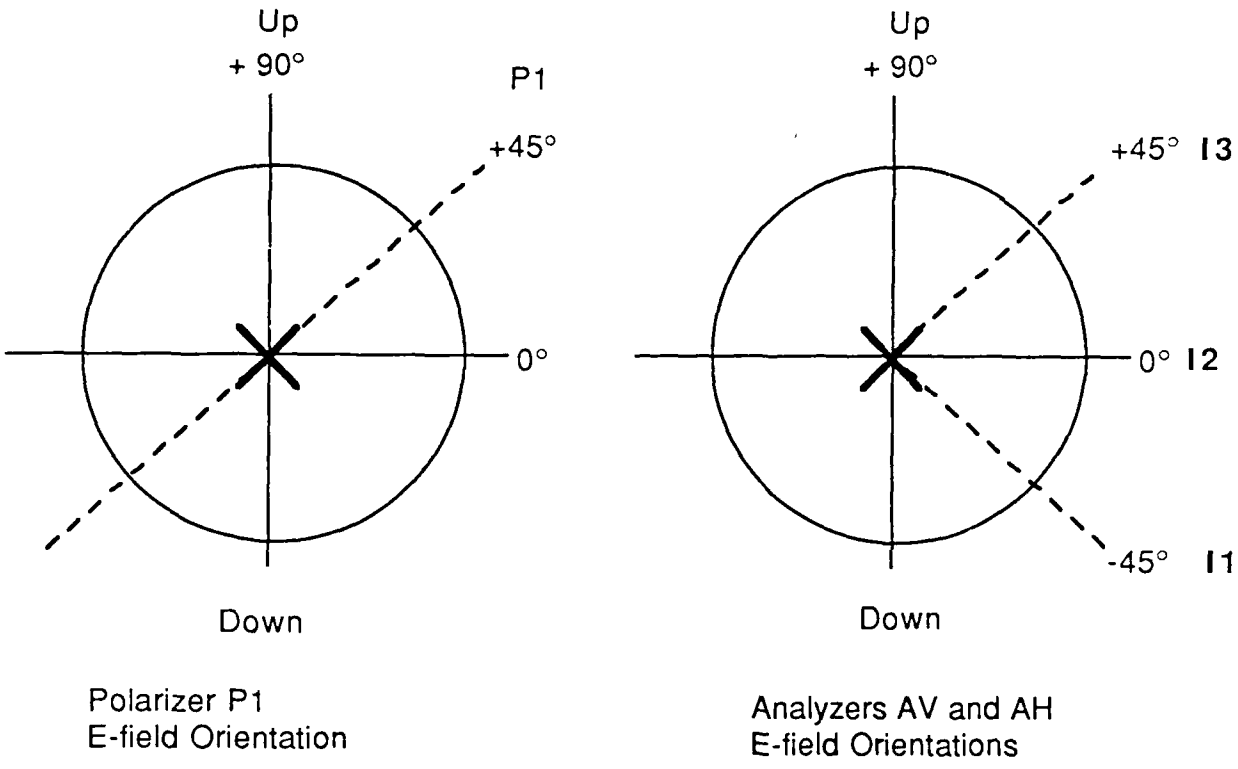


FIGURE 2. CONVENTIONS FOR THE ANGULAR ORIENTATIONS OF THE POLARIZER P1 AND THE ANALYZERS AH AND AV.

FIGURE 3. PHOTO OF SRBSE ON THE OPTICAL BENCH. The entire optical bench is enclosed in a black, wooden box. All measurements were made with the black drape covering the front opening.

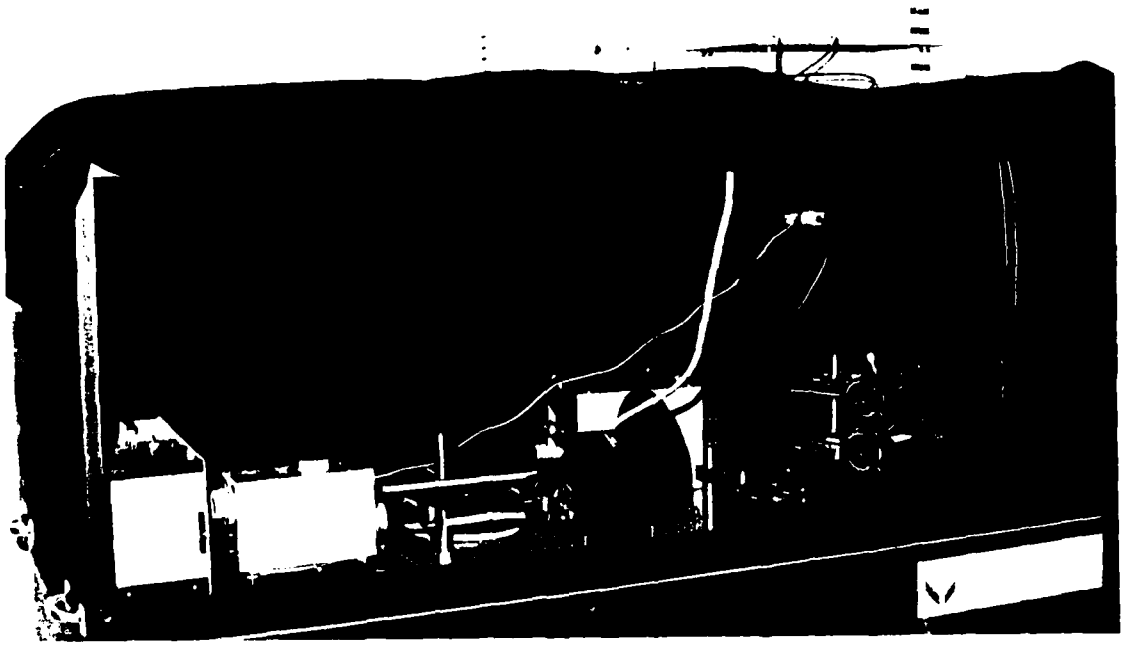

FIGURE 4. PHOTO OF THE SRBSE INSTRUMENT. Note electronics to control the chopper on the roof of the black enclosure.

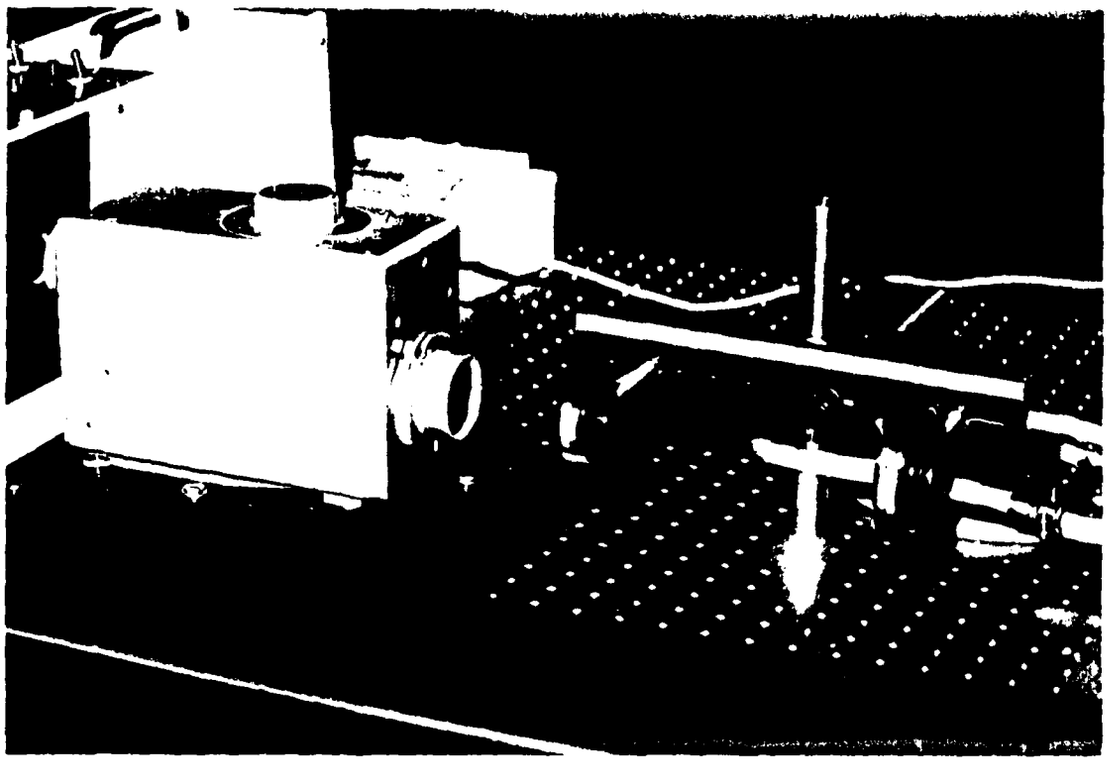

FIGURE 5. PHOTO OF THE W LAMP WITH MONOCHROMETER. After the monochrometer exit aperature is a collimator and polarizer. The polarizer was always set at 45° with respect to vertical.

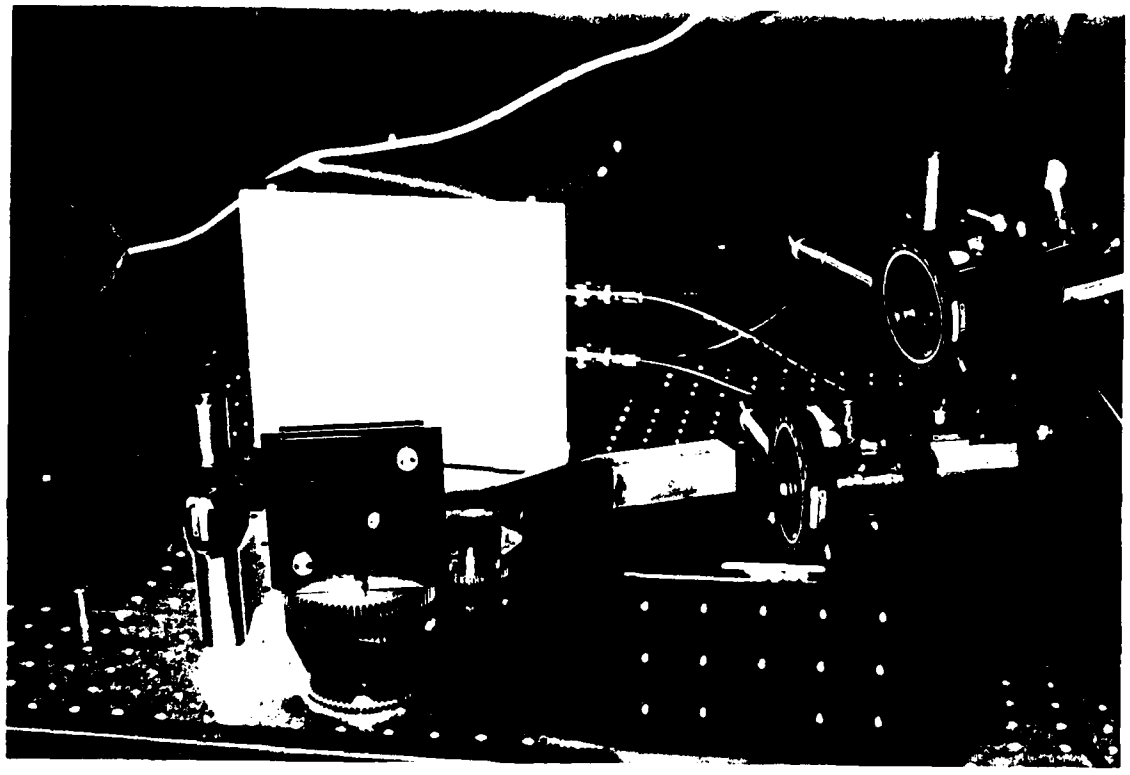

FIGURE 6. PHOTO OF THE SAMPLE HOLDER, PYRAMID AND DUAL PMT ASSEMBLY. The sample is held vertically. The samples and pyramid are on a gear mechanism to ensure that light reflected off a sample is always directed to the pyramid and PMTs regardless of angle of incidence.

The entire mechanism enabled collection of ellipsometric data over a wide range of angles of incidence data as measured with respect to the surface normal of the substrate.

The reflected beam was then directed toward a custom machined aluminum pyramid as illustrated in Figure 6. This aluminum pyramid is what makes SRBSE unique. A discussion of pyramid design and function is included in Reference 1. The reflected beam was carefully directed onto the edge between two adjacent faces on the pyramid. Each reflecting face made an angle of approximately 83° with the incident beam, which is slightly larger than the polarization (Brewster) angle for an aluminum mirror with respect to light reflected off of a silicon substrate. Had a substrate other than silicon been employed, a different pyramid geometry would have been necessary. The two adjacent faces of the pyramid were coated with evaporated aluminum in order to create a surface whose optical constants were well characterized. Great care was taken to ensure that the beam reflected off the substrate was incident directly on the corner between two adjacent faces of the pyramid, so that almost equal intensities of light were reflected off these two faces 90° apart. The "reference plane" in ellipsometry is defined by the trajectory of incident light and the reflected light. As shown in Figure 1, splitting of the reflected beam by the pyramid divided it into a horizontal component (known as in-plane or "p") and a vertical component (known as out of plane or "s"). Each beam was plane polarized by the reflecting surface to a degree that was determined by the surface material. Each beam was then directed into its own photomultiplier tube (PMT). Immediately in front of the entrance aperture of each photomultiplier tube was positioned a transmission polarizer (called an "analyzer" because of its location in the beam path) whose angular rotation of the E-field vector is described in Figure 2.

The procedure for the collection of ellipsometric data typically went as follows. First the substrate was mounted on the sample holder and the sample was tilted as needed in order to ensure the alignment of the reflected beam onto the edge of the aluminum pyramid. The alignment was indicated by measurement of almost equal intensities on both of the PMTs. The two PMT readings were monitored while the monochrometer was set to the desired wavelength. Additionally, the incident angle of light on the surface of the sample also adjusted by rotating the samples/PMT mechanical assembly. For every change in angle of incidence $\theta$ the pyramid plus PMT housing assembly was rotated by an angle $2\theta$ by the use of the 2:1 gear system. After setting the incident light wavelength and the angle of incidence, it was time to collect data. The data collected was in the form of the output reading from each of the two photomultiplier tubes. Each PMT was connected to an EG7G PARC #5104 lock-in amplifier using a #192 chopper wheel. The chopper cut the beam incident on the sample

at 1000 cycles/sec. The PMT output voltages were measured in mV and calibrated against a Keithley digital multimeter.

The analyzer on the vertical PMT was set to 45° to collect intensity I3 while the analyzer of the horizontal PMT was set at -45° to collect I1. With both analyzers 90° out of phase, the first measurement was collected. Then the vertical analyzer was then rotated to the -45° mark while the horizontal analyzer was set to +45° and measurements were repeated. Then both analyzers were rotated to the 0° mark for measurement of the final two numbers, I2. Hence, a given measurement set was composed of two PMT output voltages for three different analyzer angular orientations resulting a total of six PMT outputs. Subsequent measurements were then made by changing either the wavelength by the monochrometer or the angle of incidence $\theta$.

The entire SRBSE instrument was mounted on a vibrationally isolated optical bench made by TMC Corporation, as seen in Figure 3. Several steps were taken to minimize inaccuracies caused by stray light entering the PMTs. As shown in Figures 3 and 4, the entire top working surfacing of the optic bench was enclosed in a wooden box painted black. The front opening of the box was fitted with a removal black curtain to permit set-up of an experiment. Collection of all experimental data was performed with the curtain closed in order to exclude all room light from the PMTs. Accuracy was enhanced by use of an EG&G chopper unit which chopped the incident beam at 1000 Hz synchronized to two lock-in amplifiers to enhance the signal-to-noise ratio from the PMTs.

## 2.2 Preparation of Sample Films

Diamond Materials, Inc. prepared three different carbon films on silicon substrates for analysis by SRBSE. The diamond films were grown in DMI's proprietary plasma enhanced chemical vapor deposition reactor at substrate temperatures of 950 to 1000°C using carbon- and oxygen-containing gases diluted in $H_2$. The diamond-like carbon film was grown from a mixture of ethylene diluted in $H_2$. A 70% dense diamond film was grown on a seeded silicon substrate. Microscopy revealed the film to be composed of diamond which coated 70% of the surface whereas the remaining 30% was porosity. Finally, a fully dense polycrystalline diamond film was grown on silicon, again using seeding to enhance the nucleation density diamond on the silicon. The side of the diamond seeds used were submicron diamond powder produced by shock loading. Seeding has been found to be equivalent to scratching silicon substrates with diamond powder to enhance nucleation density. Methods have been developed to obtain fully

dense diamond films on silicon without the use of seeding or scratching. However, these methods usually entail the formation of a intermediate phase such as SiC or diamond-like carbon between the silicon substrate and the diamond coating. DMI elected not to use such an intermediate phase in order to create simple two-phase structures for ellipsometric examination instead of the more complicated three-phase structures.

# 3. RESULTS

## 3.1 Carbon Films

The diamond-like carbon film was estimated to have a thickness of less than 0.5 μm. No satisfactory SEM micrograph of this film could be obtained because of its extreme thinness, smoothness and high resistivity. Figure 7 is the Raman spectrum of this diamond-like carbon film. According to the literature [5], this film is classified as a hydrogenated diamond-like carbon film also known as a-C:H which is a hard carbon film containing > 20 atomic % hydrogen.

The 70% dense diamond film is displayed in the SEM micrographs of Figures 8 and 9. Note the large, faceted grains of diamond coalesce in certain regions but not in others. Based on these micrographs, the thickness of the diamond regions was typically ≈ 3.2 μm. Figure 10 is the Raman spectrum of the diamond portions of the 70% dense diamond film. Note the broad, sloping baseline of the spectrum which is indicative of fluorescence in the diamond film. Diamond films deposited on silicon typically have fluorescent backgrounds in their Raman spectrum because silicon impurity in diamond is thought to induce GR1 fluorescent defects. The intensity of the 1332 $cm^{-1}$ diamond peak is approximately equal to that of the 1540 $cm^{-1}$ feature attributed to $sp^2$-bonded carbon.

Figures 11 and 12 are SEM micrographs of the fully dense diamond coating. Note that the grains appear essentially the same as those in the 70% film except that the nucleation density was enhanced to the point that most of the voids between the grains were eliminated. Figure 13 is the Raman spectrum of the fully dense diamond film. Note that it is very similar to the Raman spectrum of the diamond region of the 70% diamond film.

The fourth sample to be thoroughly examined was a bare silicon wafer which was carefully cleaned before ellipsometric observation. Bare, monocrystalline silicon has been thoroughly characterized by ellipsometry with its real refractive index (n) and absorption coefficient (k) well documented as a function of wavelength. The Raman spectra of the three carbon films include the 540 $cm^{-1}$ fundamental Raman mode of the silicon substrate. No SEM micrographs were made of the bare silicon wafer because of its featureless morphology.

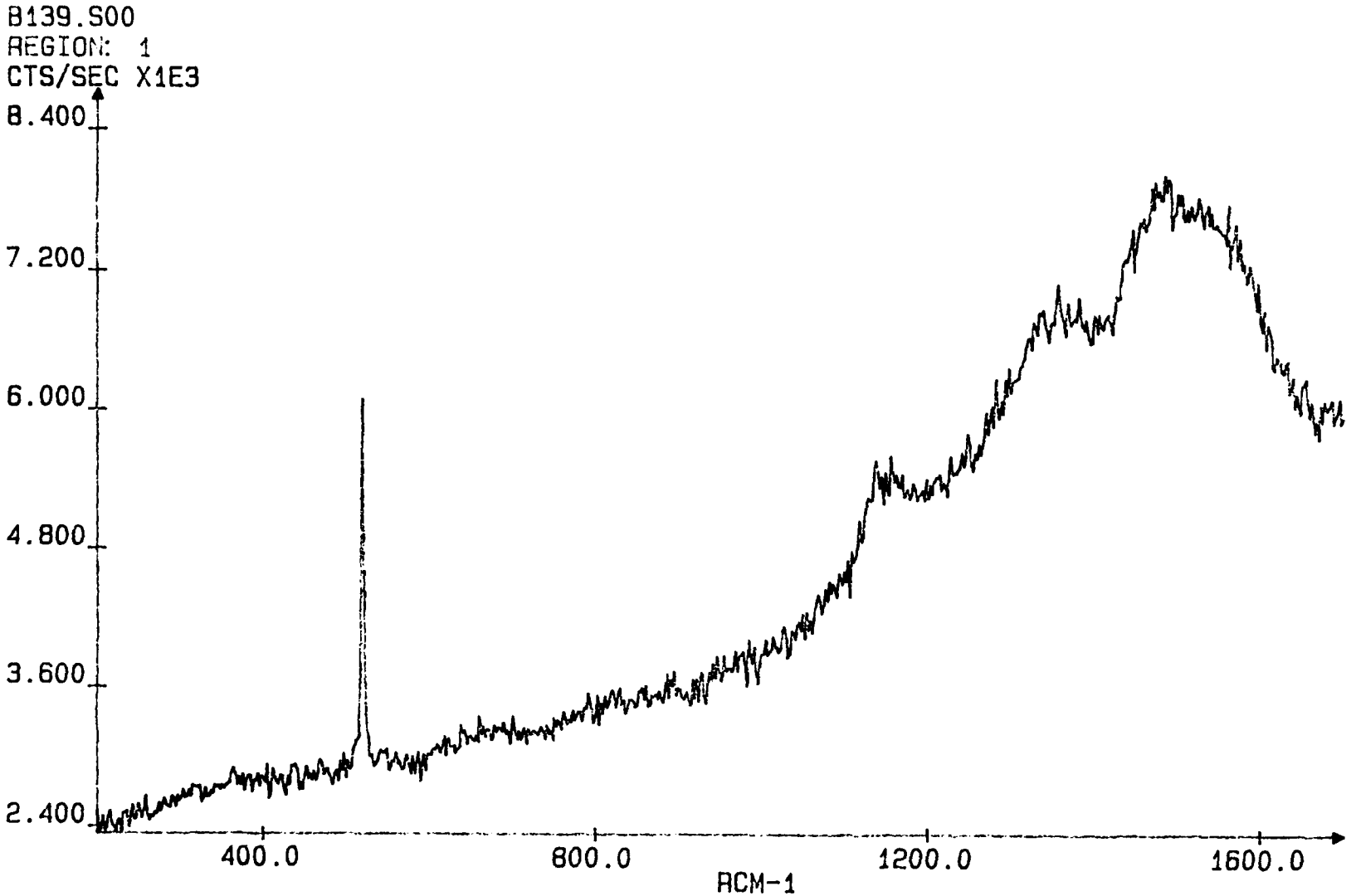


FIGURE 7. RAMAN SPECTRUM OF THE HYDROGENATED DIAMOND-LIKE CARBON FILM ON SILICON.

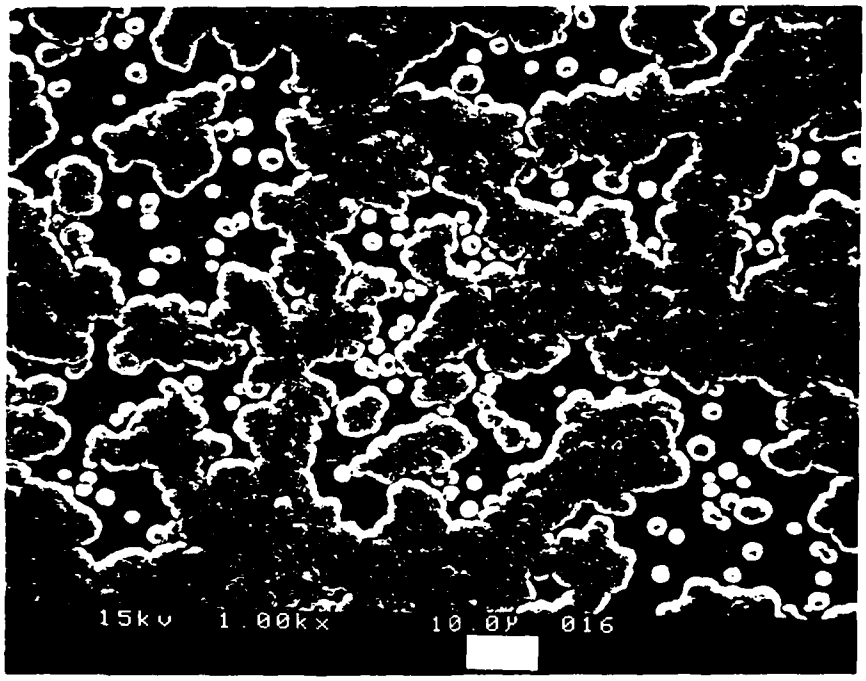


FIGURE 8. SEM MICROGRAPH OF PLAN VIEW OF 70% DENSE DIAMOND FILM ON Si.

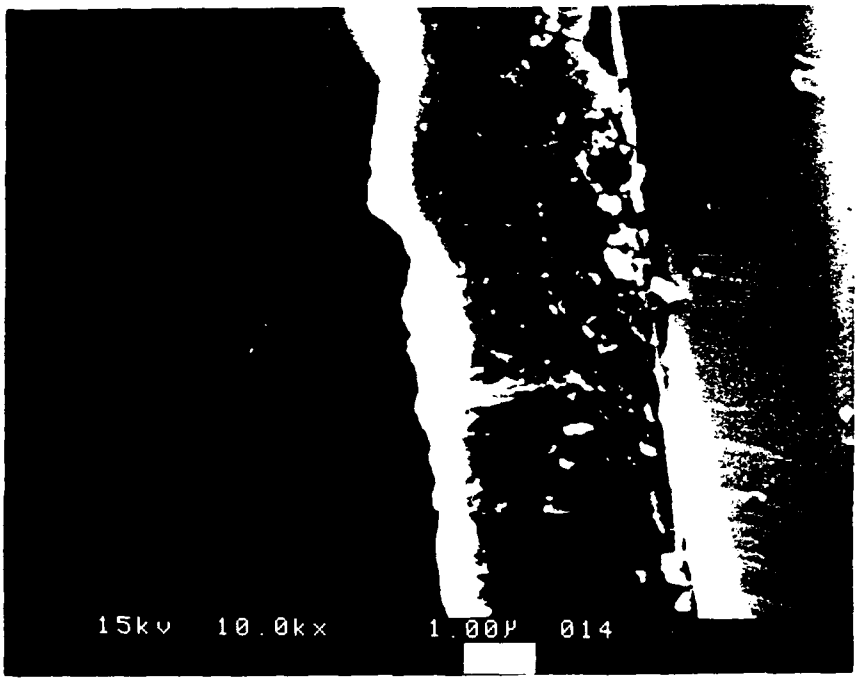


FIGURE 9. SEM MICROGRAPH OF CROSS-SECTIONAL VIEW OF 70% DENSE DIAMOND FILM ON Si. Diamond regions are 3.2 µm thick.

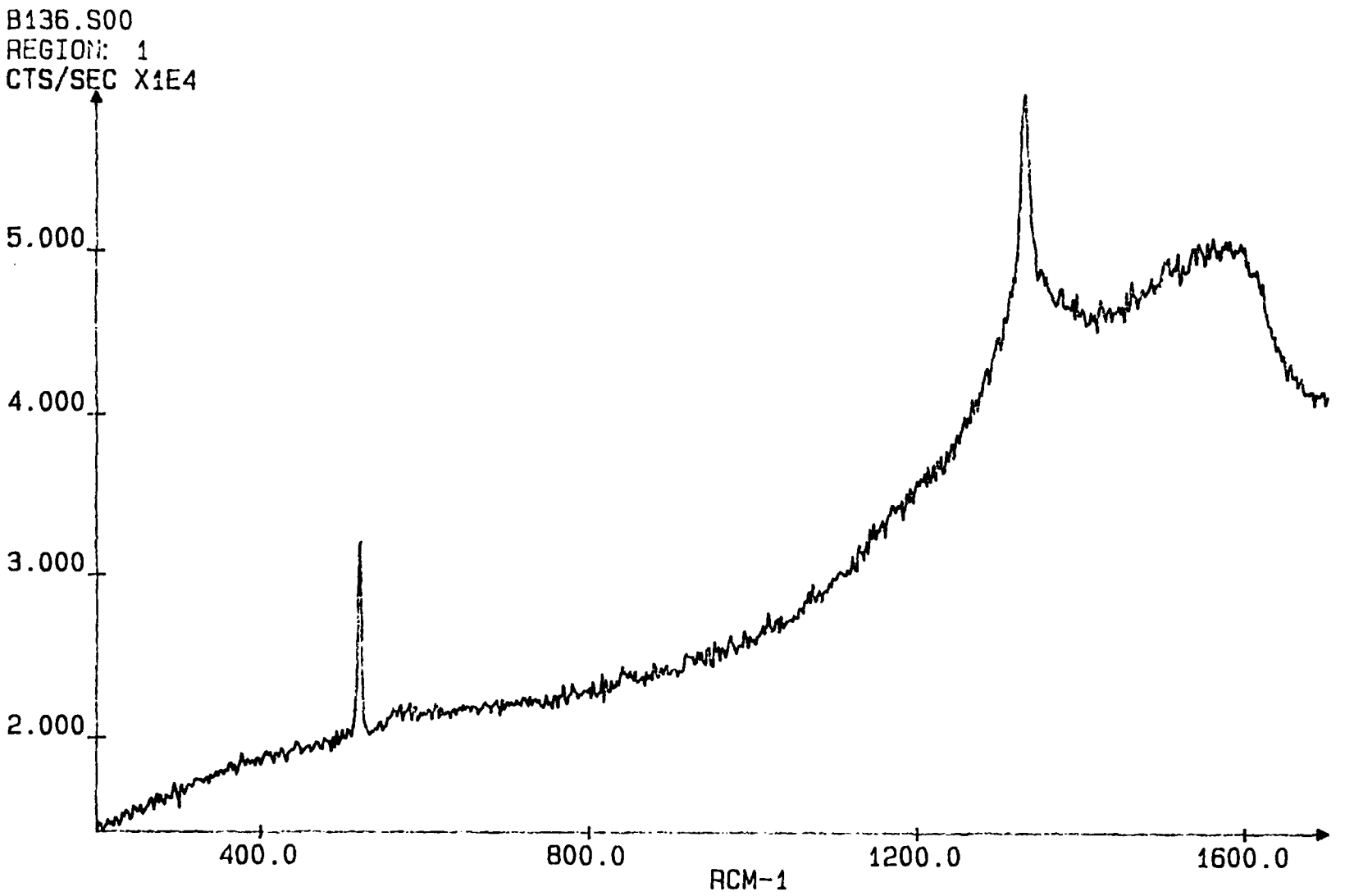


FIGURE 10. RAMAN SPECTRUM OF 70% DENSE DIAMOND FILM ON SILICON.

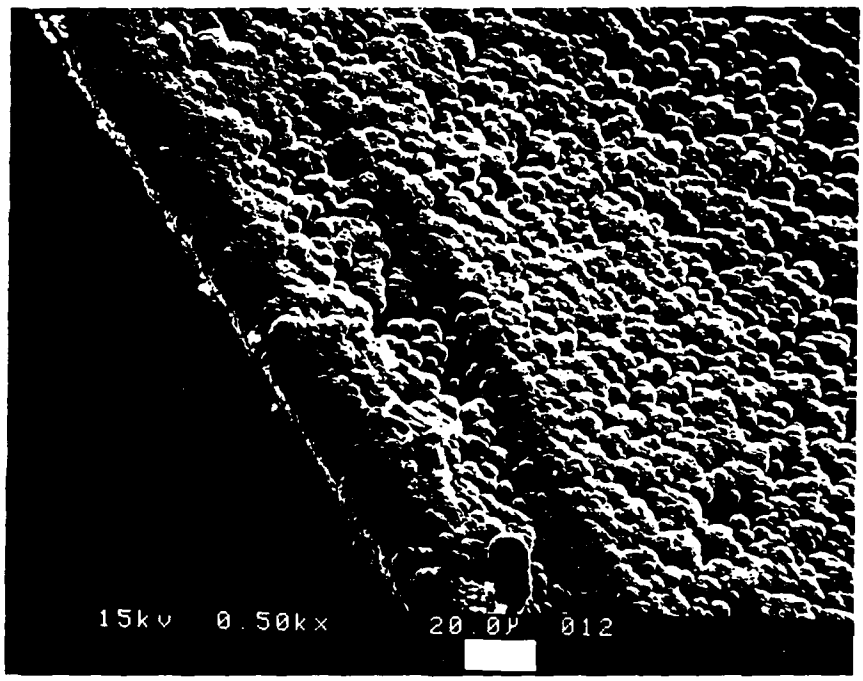


FIGURE 11. SEM MICROGRAPH OF ≈ 2.9 µm THICK, 'FULLY DENSE' DIAMOND FILM ON Si.

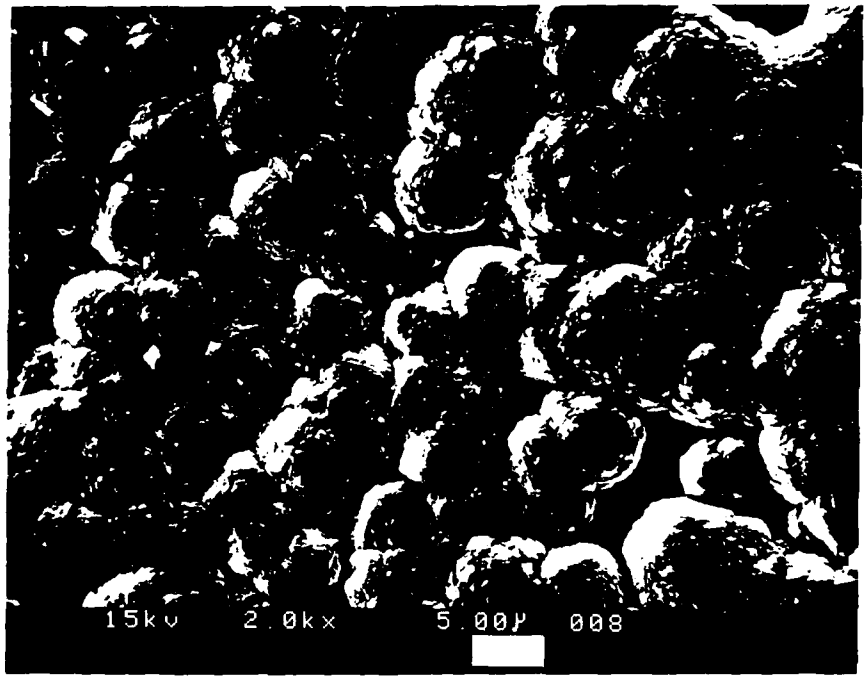


FIGURE 12. SEM MICROGRAPH OF 'FULLY DENSE' DIAMOND FILM ON Si.

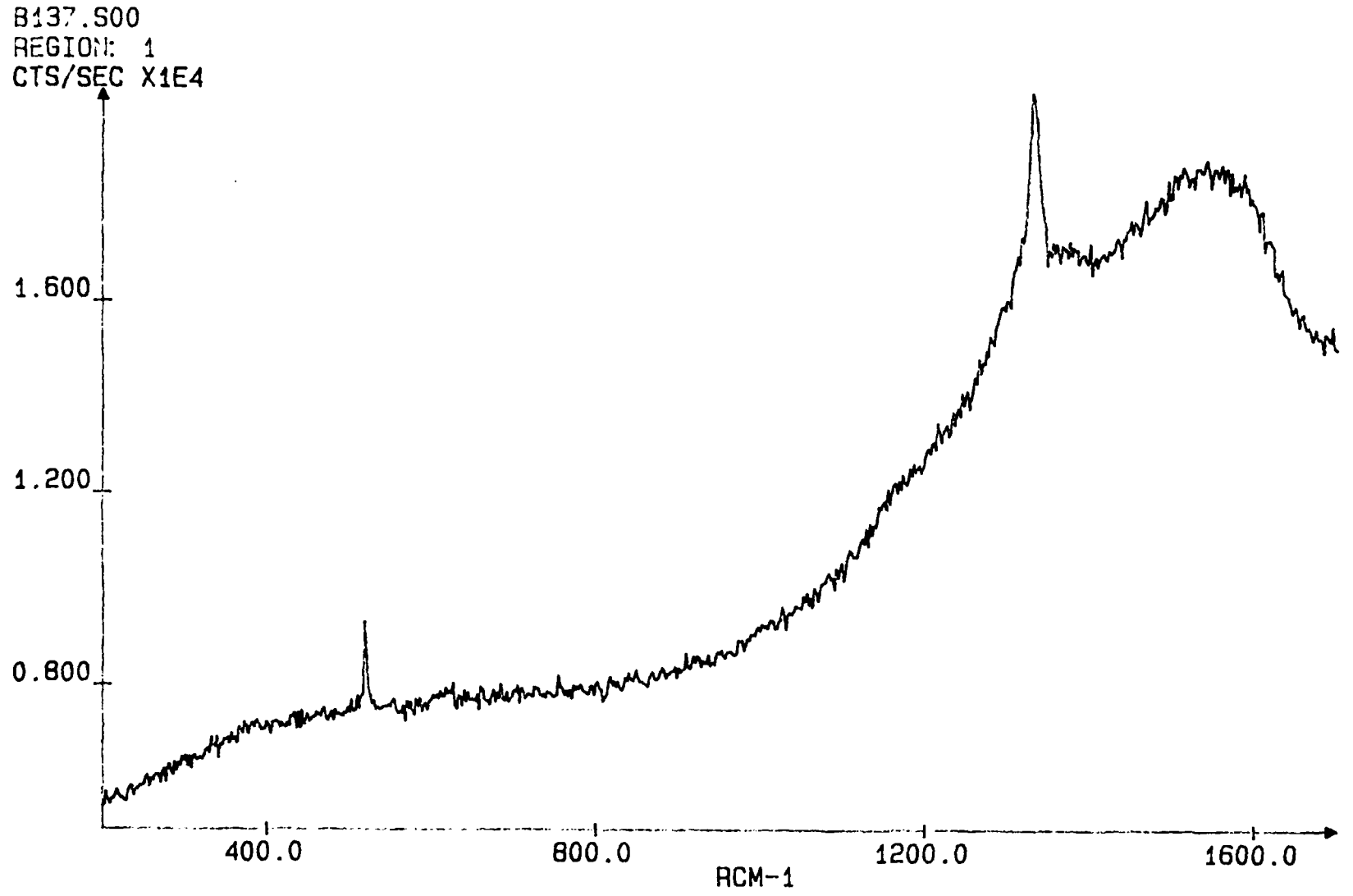


FIGURE 13. RAMAN SPECTRUM OF FULLY DENSE DIAMOND FILM ON SILICON.

## 3.2 SRBSE Results

All ellipsometry data is converted into parameters known as $\varphi$ and $\Delta$ in order to calculate optical constants of a sample.

The values of $\psi$ and $\Delta$ are determined from the intensity of the reflected beams under set conditions of the polarizer and analyzer azimuth angles, and known angle of incidence. The intensity, I, is given by

$$I = K|\tan\psi\, e^{i\Delta} \cos A \cos P \sin A \sin P|^2$$

where K is a constant, A and P are the analyzer and polarizer azimuth angles, respectively. The expressions for $\psi$ and $\Delta$ are given by

$$\psi = \tan^{-1}\,[I_2/(I_1 + I_3 - I_2)]^{1.2}$$

$$\Delta = \cos^{-1}\,[\tan\,(I_3 - I_1)/2I_2$$

where $I_1$, $I_2$, and $I_3$ are the measured intensities at analyzer azimuths of -45°, 0°, and +45°, respectively. The polarizer is fixed at +45°, and all angles are measured as positive for a counterclockwise rotation.

The equations which related n and k to the above expressions are given by $n^* = n - ik$ and for a two-phase model (ambient/substrate),

$$n = \sin\phi\,\{1 + [(1 - \rho)/(1 + \rho)]^2\tan^2\phi\}^{1/2}$$

where $\rho = \tan\psi\, e^{i\Delta}$, and $\phi$ is the angle of incidence. These are complex equations which must be separated into real and imaginary parts.

The expressions which are necessary for a three phase model (ambient/film/substrate) become more complicated. This is because reflections from the ambient/film and film/substrate interfaces interfere in phase, in addition to repeated reflections in the film. The resulting equations are deceptive in that they appear to be simple, but both n and d are implicit functions of the known parameters which makes the computations exceedingly difficult. Consequently, approximations are required which limit the calculations to two significant figures, although some of the data is not obtainable to even this precision. The necessary equations are as follows:

$$\rho = \tan\psi\, e^{i\Delta} = (r_{01p} + r_{12p}e^{-i2\delta})/(1 + 4_{01p}r_{12p}e^{-i2\delta})$$
$$(1 + r_{01s}r_{12s}e^{-i2\delta})/(r_{01s} + r^{12s}e^{-i2\delta})$$

where,

$$r_{01p} = (n_1\cos\phi_0 - n_0\cos\phi_1)/(n_1\cos\phi_0 + n_0\cos\phi_1),$$
$$r_{01s} = (n_0\cos\phi_0 - n_1\cos\phi_1)/(n_0\cos\phi_0 + n_1\cos\phi_1),$$
$$r_{12p} = (n_2\cos\phi_1 - n_1\cos\phi_2)/(n_2\cos\phi_1 + n_1\cos\phi_2),$$
$$r_{12s} = (n_1\cos\phi_1 - n_2\cos\phi_2)/(n_1\cos\phi_1 + n_2\cos\phi_2),$$
$$\delta = 2\,(d/\lambda)n_1\cos\phi_0,$$

and

$$n_0\sin\phi_0 = n_1\sin\phi_1.$$

Where $n_0$, $n_1$, and $n_2$ are the complex refractive values in the ambient, film and substrate, respectively, along with their corresponding angles of incidence of the incident beam. The wavelengths of light is given by $\lambda$.

In our case, $n_0$, $n_2$, $\phi_0$, and $\lambda$ are given, so each complex equation gives $n_1$ and d, the two unknowns. The wavelength of the light is given by $\lambda$.

The following tables are given with the calculated values for the index of refraction, $n_1 = n$ and the extinction coefficient, k, for the assumed bare silicon substrate; and for the $n = n_1$ and film thickness, d values of the various films on silicon substrate. The angle of incidence in the ambient, $\phi_0 = \phi$. Two values are shown at each wavelength. The first is that obtained by the vertical detector and the following value is that of the horizontal detector.

The accepted values for silicon are:

n = 3.88, k = .02 at $\lambda$ = 633 nm
n = 3.99, k = .03 at $\lambda$ = 580 nm
n = 4.30, k = .07 at $\lambda$ = 500 nm
n = 5.57, k = 0.4 at $\lambda$ = 400 nm

and those of diamond (cubic carbon):

$n = 2.41$ at $\lambda = 633$ nm
$n = 2.42$ at $\lambda = 580$ nm
$n = 2.42$ at $\lambda = 500$ nm
$n = 2.46$ at $\lambda = 400$ nm.

Table 1 presents the experimental data for the silicon substrate and Table 2 presents the optical constants computed from the experimental data. The average values of the refractive index, n, are compared to the accepted values for silicon with a clean surface (etched in a hydrofluoric acid bath immediately before measurement in a vacuum). The measured values at an angle of incidence of 75° were too large by roughly 10% except at 400 nm where n is too small by 20%. Nevertheless, the values do increase with decreasing wavelength as they should for silicon. The values of n should be independent of the angle of incidence although calculations showed that n became smaller as the angle of incidence decreased. In most cases, the calculated average value of the extinction coefficient, k, is larger than the accepted value. The variations in the values of n and k are understandable because of their sensitivity to $\psi$ and $\Delta$, terms which will be subsequently defined in the equations.

Note, that $\Delta$ is a sensitive function of the intensities. It can be seen from the expression that a small change in $I_2$, for example, could produce a large change in $\Delta$. In fact, for certain values of the intensities, $\Delta$ would be undefined.

The values of n for films of thickness, d, for 70% dense diamond, fully dense diamond and diamond-like carbon, each on a silicon substrate were also calculated. The experimental data is presented in Tables 3-5 and the calculated optical constants are presented in Tables 6-8. All of the films show values of n which are in the vicinity of 2.6 and $t_0$ thicknesses near 35 nm. Note that at an angle of incidence of 75°, a wavelength of 633 nm, and an index of refraction of 2.6, a calculated thickness of 35 nm could have possible values (in nm) of 35 + 130 m, where m is any positive integer. (This will become apparent from the equation for d which will be given later.) The refractive index of diamond is known to vary from 2.41 to 2.46 between 633 and 400 nm, but these values could not be resolved from our data. However, the bounded variations are random, implying a constant value for n which is consistent with our resolution. The tabulated values of n and d for different wavelengths and the corresponding values of $\psi$ and $\Delta$ are given in Tables 6-8.

TABLE 1. EXPERIMENTAL DATA FOR BARE Si WAFER.

| λ (nm) | PMT output (mV) | INCIDENT < @ 15° (⊥ 75°) I3 (+45°) | I2 (0°) | I1 (-45°) | INCIDENT < @ 22.5° (⊥ 67.5°) I3 (+45°) | I2 (0°) | I1 (-45°) | INCIDENT < @ 30° (⊥ 60°) I3 (+45°) | I2 (0°) | I1 (-45°) |
|---|---|---|---|---|---|---|---|---|---|---|
| 633 | Vv | 1.39 | 0.06 | 0.98 | 1.08 | 0.12 | 1.18 | 1.12 | 0.33 | 1.53 |
| | VH | 1.57 | 0.08 | 2.50 | 1.26 | 0.21 | 2.69 | 1.62 | 0.68 | 4.08 |
| 580 | Vv | 2.86 | 0.09 | 2.23 | 2.56 | 0.28 | 2.94 | 2.59 | 0.79 | 3.90 |
| | VH | 3.06 | 0.17 | 5.05 | 2.46 | 0.51 | 5.67 | 3.14 | 1.64 | 8.85 |
| 500 | Vv | 4.85 | 0.15 | 4.07 | 4.46 | 0.76 | 7.01 | 4.24 | 1.60 | 2.61 |
| | VH | 4.40 | 0.35 | 7.95 | 3.39 | 1.30 | 10.78 | 4.20 | 3.19 | 5.03 |
| 400 | Vv | 1.18 | 0.17 | 1.29 | 1.29 | 0.48 | 2.22 | 1.10 | 0.73 | 2.54 |
| | VH | 0.81 | 0.26 | 2.21 | 0.78 | 0.67 | 3.11 | 0.93 | 1.36 | 4.47 |

TABLE 2. SILICON (no oxide).

| Angle of Incidence $\phi$, (deg)* | Wavelength nm ** | $\psi$ (deg) | $\Delta$ (deg) | n | k |
|---|---|---|---|---|---|
| 75.0 | 633 | 3.72 | 178 | 4.22 | 0 |
| 75.0 | 633 | 4.92 | 177 | 4.39 | 0 |
| 75.0 | 580 | 5.08 | 179 | 4.41 | 0 |
| 75.0 | 580 | 7.00 | 179 | 4.71 | 0 |
| 75.0 | 500 | 6.08 | 114 | 3.97 | .740 |
| 75.0 | 500 | 8.96 | 180 | 5.05 | 0 |
| 75.0 | 400 | 13.3 | 89.5 | 3.33 | 1.55 |
| 75.0 | 400 | 15.3 | 148 | 5.54 | 1.69 |
| 67.5 | 633 | 10.2 | 105 | 2.46 | .771 |
| 67.5 | 633 | 11.6 | 110 | 2.52 | .896 |
| 67.5 | 580 | 11.6 | 102 | 2.39 | .874 |
| 67.5 | 580 | 13.8 | 150 | 3.42 | .833 |
| 67.5 | 500 | 14.4 | 119 | 2.69 | 1.16 |
| 67.5 | 500 | 17.3 | 159 | 4.01 | .941 |
| 67.5 | 400 | 20.5 | 117 | 2.61 | 1.77 |
| 67.5 | 400 | 23.5 | 149 | 4.16 | 2.21 |
| 60.0 | 633 | 19.0 | 113 | 1.72 | 1.01 |
| 60.0 | 633 | 19.6 | 134 | 2.21 | 1.14 |
| 60.0 | 580 | 19.7 | 110 | 1.64 | 1.03 |
| 60.0 | 580 | 21.5 | 135 | 2.24 | 1.32 |
| 60.0 | 500 | 21.1 | 117 | 1.74 | 1.18 |
| 60.0 | 500 | 23.8 | 140 | 2.44 | 1.57 |
| 60.0 | 400 | 25.6 | 123 | 1.75 | 1.59 |
| 60.0 | 400 | 29.5 | 142 | 2.46 | 2.36 |

The average values n and k are:

When $\phi = 75°$

n = 4.30, k = 0; at 633 nm
n = 4.40, k = 0; at 580 nm
n = 4.51, k = 0.368; at 500 nm
n = 4.44, k = 1.62; at 400 nm

TABLE 2 (Continued)

When $\phi = 67.5°$

n = 2.49, k = .833; at 633 nm
n = 2.91, k = .853; at 580 nm
n = 3.35, k = 1.05; at 500 nm
n = 3.39, k = 1.99; at 400 nm

When $\phi = 60°$

n = 1.97, k = 1.08; at 633 nm
n = 1.94, k = 1.18; at 580 nm
n = 2.09, k = 1.38; at 500 nm
n = 2.11, k = 1.98; at 400 nm

* Note that a small change in $\phi$ can significantly change the value of n. For instance, if $\phi$ is 74.0° then n = 3.94 at 633 nm.

** The value of $\Delta$ can change both n and k even when $\psi$ is fixed. At 67.5° and 633 nm, n = 3.34, k = 0 if $\psi = 10.2$ and $\Delta = 180$. Also, at 60°, and 400 nm, n = 5.46, k = 0. 746 when $\psi$ = 24.1 and $\Delta = 175$. These values should be compared with the values in Table 1.

TABLE 3. EXPERIMENTAL DATA FOR HYDROGENATED DLC FILM ON Si.

| λ (nm) | PMT output (mV) | INCIDENT < @ 15° (⊥ 75°) I3 (+45°) | I2 (0°) | I1 (-45°) | INCIDENT < @ 22.5° (⊥ 67.5°) I3 (+45°) | I2 (0°) | I1 (-45°) | INCIDENT < @ 30° (⊥ 60°) I3 (+45°) | I2 (0°) | I1 (-45°) |
|---|---|---|---|---|---|---|---|---|---|---|
| 633 | Vv | 2.01 | 0.08 | 1.38 | 1.60 | 0.18 | 1.56 | 1.42 | 0.40 | 1.82 |
| | VH | 2.49 | 0.20 | 4.48 | 2.01 | 0.43 | 4.77 | 1.78 | 0.77 | 4.87 |
| 580 | Vv | 4.08 | 0.17 | 2.80 | 3.54 | 0.42 | 3.60 | 2.88 | 0.91 | 3.95 |
| | VH | 4.70 | 0.44 | 8.87 | 3.79 | 1.02 | 9.92 | 3.25 | 1.79 | 10.11 |
| 500 | Vv | 7.38 | 0.36 | 1.76 | 6.13 | 0.98 | 2.38 | 4.89 | 1.82 | 2.69 |
| | VH | 6.84 | 0.90 | 4.85 | 5.17 | 2.25 | 5.62 | 4.34 | 3.63 | 5.91 |
| 400 | Vv | 2.00 | 0.31 | 1.70 | 1.64 | 0.57 | 2.27 | 1.28 | 0.78 | 2.47 |
| | VH | 1.28 | 0.57 | 4.17 | 0.98 | 1.09 | 4.79 | 0.86 | 1.48 | 4.90 |

TABLE 4. EXPERIMENTAL DATA FOR 70% DENSE DIAMOND FILM ON Si.

| λ (nm) | PMT output (mV) | INCIDENT < @ 15° (⊥ 75°) I3 (+45°) | I2 (0°) | I1 (-45°) | INCIDENT < @ 22.5° (⊥ 67.5°) I3 (+45°) | I2 (0°) | I1 (-45°) | INCIDENT < @ 30° (⊥ 60°) I3 (+45°) | I2 (0°) | I1 (-45°) |
|---|---|---|---|---|---|---|---|---|---|---|
| 633 | Vv | 1.80 | 0.44 | 0.70 | 0.88 | 0.14 | 0.40 | 0.87 | 0.17 | 0.72 |
| | VH | 6.09 | 0.97 | 3.91 | 3.46 | 0.34 | 3.08 | 1.61 | 0.42 | 3.36 |
| 580 | Vv | 3.71 | 0.91 | 1.16 | 1.78 | 0.29 | 0.76 | 1.78 | 0.42 | 1.51 |
| | VH | 12.18 | 2.03 | 6.66 | 6.31 | 0.71 | 5.40 | 2.92 | 0.94 | 6.63 |
| 500 | Vv | 1.79 | 1.46 | 1.58 | 3.02 | 0.47 | 1.63 | 3.63 | 0.90 | 3.91 |
| | VH | 5.19 | 2.97 | 7.86 | 8.63 | 1.05 | 7.85 | 4.31 | 1.72 | 11.38 |
| 400 | Vv | 1.30 | 0.35 | 0.36 | 0.75 | 0.19 | 0.50 | 1.00 | 0.43 | 1.33 |
| | VH | 3.40 | 0.69 | 1.52 | 1.55 | 0.33 | 1.77 | 0.90 | 0.71 | 3.11 |

TABLE 5. EXPERIMENTAL DATA FOR FULLY DENSE DIAMOND FILM ON Si.

| λ (nm) | PMT output (mV) | INCIDENT < @ 15° (⊥ 75°) I3 (+45°) | I2 (0°) | I1 (-45°) | INCIDENT < @ 22.5° (⊥ 67.5°) I3 (+45°) | I2 (0°) | I1 (-45°) | INCIDENT < @ 30° (⊥ 60°) I3 (+45°) | I2 (0°) | I1 (-45°) |
|---|---|---|---|---|---|---|---|---|---|---|
| 633 | Vv | 0.33 | 0.10 | 0.12 | 0.20 | 0.04 | 0.08 | 0.10 | 0.03 | 0.07 |
| | VH | 1.46 | 0.24 | 0.74 | 0.87 | 0.06 | 0.57 | 0.26 | 0.01 | 0.32 |
| 580 | Vv | 0.72 | 0.22 | 0.20 | 0.43 | 0.08 | 0.16 | 0.21 | 0.04 | 0.14 |
| | VH | 2.92 | 0.50 | 1.30 | 1.71 | 0.14 | 1.06 | 0.55 | 0.03 | 0.62 |
| 500 | Vv | 1.40 | 0.37 | 0.30 | 0.76 | 0.13 | 0.26 | 0.38 | 0.05 | 0.23 |
| | VH | 4.51 | 0.78 | 1.72 | 2.35 | 0.21 | 1.43 | 0.78 | 0.06 | 0.87 |
| 400 | Vv | 0.28 | 0.10 | 0.07 | 0.16 | 0.04 | 0.07 | 0.09 | 0.03 | 0.06 |
| | VH | 0.87 | 0.18 | 0.33 | 0.40 | 0.05 | 0.25 | 0.14 | 0.01 | 0.16 |

TABLE 6. DIAMOND-LIKE CARBON ON SILICON.

| Wavelength (nm) | ψ (deg) | Δ (deg) | n | d* (nm) | |
|---|---|---|---|---|---|
| | | | | | $\phi = 75°$ |
| 633 | 7.6 | 58 | 3.0 | 43 | |
| 633 | 8.4 | 43 | 3.0 | 46 | |
| 580 | 7.9 | 58 | 3.0 | 40 | |
| 580 | 9.2 | 39 | 2.9 | 44 | |
| 500 | 8.8 | 63 | 3.0 | 34 | |
| 500 | 10 | 38 | 2.9 | 39 | |
| 400 | 15 | 83 | 2.7 | 20 | |
| 400 | 16 | 42 | 2.7 | 29 | |
| | | | | | $\phi = 67.5°$ |
| 633 | 12 | 89 | 2.9 | 35 | |
| 633 | 13 | 44 | 2.8 | 48 | |
| 580 | 12 | 89 | 2.8 | 34 | |
| 580 | 14 | 43 | 2.8 | 44 | |
| 500 | 14 | 83 | 2.8 | 27 | |
| 500 | 16 | 41 | 2.7 | 38 | |
| 400 | 19 | 79 | 2.7 | 22 | |
| 400 | 22 | 45 | 2.4 | 33 | |
| | | | | | $\phi = 60°$ |
| 633 | 18 | 81 | 2.4 | 39 | |
| 633 | 17 | 52 | 2.6 | 47 | |
| 580 | 19 | 79 | 2.8 | 30 | |
| 580 | 37 | Indeterminate | | | |
| 500 | 38 | 48 | 2.0 | 54 | |
| 500 | 21 | 46 | 2.5 | 38 | |
| 400 | 32 | 61 | 2.0 | 40 | |
| 400 | 26 | 48 | 2.2 | 36 | |

* d = 37 nm at 75°
d = 35 nm at 67.5°
d = 41 nm at 60°

TABLE 7. 70% DENSE DIAMOND FILM ON SILICON.

| Wavelength (nm) | ψ (deg) | Δ (deg) | n | d* (nm) | |
|---|---|---|---|---|---|
| | | | | | $\phi = 75°$ |
| 633 | 21 | 61 | 2.3 | 42 | |
| 633 | 16 | 72 | 2.6 | 36 | |
| 580 | 15 | 68 | 2.6 | 27 | |
| 580 | 14 | 70 | 2.7 | 32 | |
| 500 | 26 | 42 | 2.4 | 45 | |
| 500 | 24 | 44 | 2.4 | 45 | |
| 400 | 24 | 53 | 2.3 | 37 | |
| 400 | 19 | 62 | 2.5 | 29 | |
| | | | | | $\phi = 67.5°$ |
| 633 | 17 | 59 | 2.7 | 39 | |
| 633 | 13 | 83 | 2.6 | 33 | |
| 580 | 17 | 57 | 2.6 | 40 | |
| 580 | 12 | 82 | 2.7 | 32 | |
| 500 | 16 | 65 | 2.6 | 32 | |
| 500 | 13 | 85 | 2.7 | 25 | |
| 400 | 20 | 76 | 2.8 | 24 | |
| 400 | 16 | 85 | 2.6 | 21 | |
| | | | | | $\phi = 60°$ |
| 633 | 17 | 82 | 2.6 | 29 | |
| 633 | 15 | 57 | 2.7 | 42 | |
| 580 | 18 | 84 | 2.8 | 31 | |
| 580 | 16 | 56 | 2.7 | 42 | |
| 500 | 17 | 87 | 2.4 | 32 | |
| 500 | 17 | 52 | 2.6 | 37 | |
| 400 | 22 | 81 | 2.0 | 25 | |
| 400 | 21 | 53 | 2.4 | 32 | |

* The average value of d, d should be independent of wavelength and angle of incidence. Although the values of d vary, the average at the different incident angles does not change much considering our data.

The values of d are:

$d = 37$ nm when $\phi = 75°$

$d = 31$ nm when $\phi = 67.5°$

$d \simeq 34$ nm when $\phi = 60°$

TABLE 8. FULLY DENSE DIAMOND FILM ON SILICON.

| Wavelength (nm) (deg) | ψ (deg) | Δ | n | d* (nm) | |
|---|---|---|---|---|---|
| | | | | | $\phi = 75°$ |
| 633 | 24 | 62 | 2.2 | 44 | |
| 633 | 17 | 63 | 2.6 | 47 | |
| 580 | 25 | 56 | 2.3 | 40 | |
| 580 | 17 | 60 | 2.6 | 40 | |
| 500 | 24 | 49 | 2.4 | 39 | |
| 500 | 18 | 55 | 2.6 | 35 | |
| 400 | 28 | 57 | 2.2 | 37 | |
| 400 | 20 | 58 | 2.5 | 30 | |
| | | | | | $\phi = 67.5°$ |
| 633 | 19 | 59 | 2.5 | 45 | |
| 633 | 10 | 63 | 2.9 | 42 | |
| 580 | 19 | 55 | 2.5 | 42 | |
| 580 | 11 | 63 | 2.9 | 36 | |
| 500 | 18 | 51 | 2.6 | 35 | |
| 500 | 12 | 63 | 2.8 | 32 | |
| 400 | 21 | 64 | 2.7 | 26 | |
| 400 | 14 | 67 | 2.6 | 25 | |
| | | | | | $\phi = 60°$ |
| 633 | 23 | 78 | 2.2 | 39 | |
| 633 | 6.5 | 70 | 3.2 | 40 | |
| 580 | 33 | 55 | 2.0 | 58 | |
| 580 | 8.5 | 80 | 3.0 | 34 | |
| 500 | 15 | 67 | 2.6 | 31 | |
| 500 | 9.5 | 83 | 2.5 | 32 | |
| 400 | 17 | 81 | 2.4 | 25 | |
| 400 | 15 | 75 | 2.6 | 25 | |

* d = 39 nm at 75°
d = 35 nm at 67.5°
d = 36 nm at 60°

The ellipsometric calculations were made for data taken for each of the two beams with the intent that any variations of the incident intensity during the measurements would not affect the final determination of the optical constants. The results show that variations in the data were too large for the technique to be meaningful. This can be seen by inspecting the vertical and horizontal values of the optical constants, n and k, at each wavelength. However, it should be emphasized that the usefulness of the technique is masked by the inaccuracy in the measurements. Even with these large differences between the vertical and horizontal values, when the optical constants are to be determined, the technique essentially yields the average value at each wavelength.

## 4. DISCUSSION

The values of n and k for silicon were calculated by accounting for the variation of 0.05 mV in the measured data. The values of the measured data were modified for calculations assuming this error. The approach was an optimization procedure in an attempt to obtain the best fit for n and k at all the angles of incidence. These are the values given which are given in Table 2.

The raw data at 75° gives values of n which range from 3.69 at 633 nm to 3.40 at 400 nm. (These calculations are available if required but are not part of this report, nor are many of the other trials for values which were used in an effort to optimize the results.) Clearly a better fit to the accepted value of 3.88 at the longer wavelength, but in serious disagreement at the short wavelength where the book value is 5.57. The values of n at 67.5° and 60° were 2.27 and 1.43, respectively, at the long wavelength, and decreased to as low as 1.06 at 400 nm. The values of k were all too high approaching a value of 1.0 at 633 nm, which is also unreasonable.

The results for the three phase models of graphite/silicon, diamond/silicon, and diamond-like carbon/silicon are dependent on the same sensitive functions of $\psi$ and $\Delta$. Some approximations were required here in order to facilitate the calculations. The computations were restricted to two significant figures and the value of k for the film was considered to be zero. While this assumption may be true for the diamond film over the wavelength range it may not be for the others. The equations, however, are valid even when k is not zero, but, then the calculations become unmanageable without extensive computer aid.

The values of d for the three phase models is cyclical and repeats with every 180° phase change in $\delta$. As discussed earlier, this means that the calculated value for d of 35 nm could have values increased by an integral of 130 nm when measurements are made at 75° and wavelength of 633 nm.

The purpose of the silicon sample was for its use in the calibration process. The information obtained from the analysis and its results indicates that factors affecting the systematic errors have to be addressed. Some of the factors are:

1. Although, the beam divider can give values for the vertical and horizontal detectors which are different (which is permissible), the values are too different, which is indicative of poor surface reflectance, misalignment, or both. Further, the ratio of $I_3$ to $I_1$ for the vertical detector, for example,

changes by 56% (from 400-633 nm) which is not consistent with the ratio for earlier data (not used) which changed by 26% for the same wavelength range.

2. Either the light intensity must be increased or the experiment must be capable of reliable measurements under low light conditions. Then the incident beam can be made more monochromatic. This may be the most significant improvement that can be made. The data taken under the present conditions indicate that the incident beam was not sufficiently monochromatic for our requirements.

3. The condition of the incident light plays a major role in determining the critical values of $\psi$ and $\Delta$. It is therefore necessary that the polarizer and analyzer azimuths be known accurately, but more significantly, that the state of the light be linearly polarized after passing through the polarizer. The data indicate that the light passing through the polarizer was not linearly polarized, although a good quality polarizer was used.

4. The preparation of the silicon sample surface is important in determining its optical constants. To maximize accuracy, the silicon surface must be cleaned of contaminants before measurement. When these steps are not taken, then complicated models must be assumed in order to account for the surface artifacts. However, the other three requirements indicated above must be addressed before any significant change due to surface effects can be discerned.

In summary, it appears that it is necessary to refine the experimental technique in order to obtain the resolution required for our materials. Considering the limited time spent for the measurements, and the experimental difficulties, the results were better than expected, realizing that many of the calculations could have been indeterminate had there been gross inaccuracies in the measured data. This, however, was not the case.

Although the effort expended for the analyses and calculations of the different models exceeded expectations, the project was worthwhile, considering that the results under the circumstances are encouraging.

## 5. CONCLUSIONS

Split reflected beam spectroscopic ellipsometry is a new method of collecting ellipsometric data which requires further work in order to obtain reliable and accurate data. Although the hardware costs associated with setting up an SRBSE unit are a factor of two less than the hardware costs of a commercial spectroscopic ellipsometer, the time and effort required to obtain accurate results are severe since numerous practical problems must be solved. Dr. Russo related that it took him several years in order to get his SRBSE perfected to the point where he obtained accurate results when examining $SiO_2$ films on silicon. The Principal Investigator and technical workers on this program feel that with further time and effort, accurate results could have been obtained by further modifying the SRBSE unit assembled for this Phase I program. For example, the intensity and monochromaticity problem could be solved by using a tunable die laser instead of the lamp + monochrometer combination. However, an tunable die laser would render the SRBSE instrument very expensive, and would be certainly outside the budget of an SBIR Phase I program.

This program identified several instrumental sources of error, including low beam intensity, possible beam divergence, and insufficient monochrometicity of the beam. Because of these problems, it is concluded that SRBSE has many problems which must be overcome to be suitable as a benchtop technique. Only after these problems can be routinely overcome can it be worth considering the question of suitability for *in situ* ellipsometry in CVD chambers.

The Principal Investigator believes that SRBSE does have great promise as a benchtop alternative to conventional spectroscopic ellipsometers, but some organization other than Diamond Materials, Inc. must be willing to invest the engineering time and effort involved into realizing that goal. In the meantime, Raman spectroscopy remains the most reliable and accurate method of distinguishing between the various allotropes of carbon with ellipsometry being more suited for *in situ* studies using sophisticated state-of-the-art equipment.

Since the proposal for this program was written (December 1987), the state-of-the-art in diamond thin-film growth has improved to the point that diamond thin-film growth reproducibility is now outstanding. *In situ* monitoring tools such as *in situ* ellipsometry are only economically justifiable for research and development purposes or to understand the fundamental science and kinetics of diamond film growth. DMI, being a for-profit advanced materials company, cannot imagine needing *in situ* ellipsometry or Raman spectroscopy to monitor film deposition as a routine QA tool. It

remains much more easier and cost effective to analyze all diamond film *ex situ* using Raman spectroscopy and SEM rather than going through the effort, time, and cost to attempt *in situ* measurements. In the past two years of existence, DMI has not noted any other companies in diamond attempting *in situ* measurements of film quality since film reproducibility is very good. Such *in situ* techniques for diamond growth would only be justifiable in production if and when highly sophisticated techniques such as atomic layer epitaxy are routinely employed for the epitaxial growth of diamond thin-films.

REFERENCES


1. O. L. Russo, "An Accurate Ellipsometric Reflectance Ratio Method," *J. Phys. D.:Appl. Phys.* **18** 1723 (1985).

2. R. W. Collins, "Surface, Interface, and Bulk Properties of Amorphous Carbon Films Characterized by In Situ Ellipsometry," Appl. Phys. Lett. 52, 9240, 2025 (1988).

3. R. W. Collins, Y. Cong, Y. T. Kim, K. Vedam, Y. Liou, A. Inspektor, and R. Messier, "Real Time Spectroscopic Ellipsometry Characterization of Diamond and Diamond Like Films," to be published in *Thin Solid Films* (1989).

4. R. W. Collins, "Real Time Ellipsometry Characterization and Process Monitoring for Amorphous Carbon Deposition," in Preparation and Characterization of Amorphous Diamond Films, edited by J. Pouch and S. Alterovitz, Trans Tech Publications, Aedermannsdorf, Switzerland (in press).

5. D. S. Knight and W. B. White, "Characterization of Diamond Films by Raman Spectroscopy," *Journal of Materials Research*, 4 [2] 385 (1989).